Oral Radiology (2019) 35:143–151
https://doi.org/10.1007/s11282-018-0330-3

ORIGINAL ARTICLE

Improvement of region of interest extraction and scanning method of computer-aided diagnosis system for osteoporosis using panoramic radiographs

Takashi Nakamoto[1] · Akira Taguchi[2] · Rinus Gerardus Verdonschot[3] · Naoya Kakimoto[3]

Received: 18 January 2018 / Accepted: 5 April 2018 / Published online: 25 April 2018

Abstract

Objectives Patients undergoing osteoporosis treatment benefit greatly from early detection. We previously developed a computer-aided diagnosis (CAD) system to identify osteoporosis using panoramic radiographs. However, the region of interest (ROI) was relatively small, and the method to select suitable ROIs was labor-intensive. This study aimed to expand the ROI and perform semi-automatized extraction of ROIs. The diagnostic performance and operating time were also assessed.

Methods We used panoramic radiographs and skeletal bone mineral density data of 200 postmenopausal women. Using the reference point that we defined by averaging 100 panoramic images as the lower mandibular border under the mental foramen, a 400 × 100-pixel ROI was automatically extracted and divided into four 100 × 100-pixel blocks. Valid blocks were analyzed using program 1, which examined each block separately, and program 2, which divided the blocks into smaller segments and performed scans/analyses across blocks. Diagnostic performance was evaluated using another set of 100 panoramic images.

Results Most ROIs (97.0%) were correctly extracted. The operation time decreased to 51.4% for program 1 and to 69.3% for program 2. The sensitivity, specificity, and accuracy for identifying osteoporosis were 84.0, 68.0, and 72.0% for program 1 and 92.0, 62.7, and 70.0% for program 2, respectively. Compared with the previous conventional system, program 2 recorded a slightly higher sensitivity, although it occasionally also elicited false positives.

Conclusions Patients at risk for osteoporosis can be identified more rapidly using this new CAD system, which may contribute to earlier detection and intervention and improved medical care.

Keywords Diagnostic imaging · Osteoporosis · Radiography · Mandible

Introduction

Osteoporosis is a disease characterized by low bone mass and micro-architectural deterioration of bone tissue, leading to increased bone fragility and a consequent higher risk of fracture [1]. Given that osteoporosis typically occurs in the older adult population, a significant surge in its occurrence in Japan can be foreseen owing to the high proportion of elderly individuals among Japanese citizens. A report by the International Osteoporosis Foundation estimated that approximately 10% of Japanese individuals aged ≥ 40 years are osteoporotic (i.e., 3.0 million men and 9.8 million women), representing a significant impact on healthcare resources and treatment costs [2]. Early intervention is particularly important to alleviate discomfort in patients at risk of osteoporosis and diminish the burden on the healthcare system. Individuals at particularly high risk of developing fractures from osteoporosis are postmenopausal women with low skeletal bone mineral density (BMD). Therefore, the importance of screening postmenopausal women with a high risk of osteoporosis has been reported in many past studies [3–9]. Bone mass measurement, such as that performed by dual-energy X-ray absorptiometry (DXA), is considered the most reliable procedure to identify low BMD before the incidence of

✉ Takashi Nakamoto
tnk@hiroshima-u.ac.jp

1 Department of Oral and Maxillofacial Radiology, Hiroshima University Hospital, 1-2-3 Kasumi, Minami-ku, Hiroshima 734-8553, Japan

2 Department of Oral and Maxillofacial Radiology, Matsumoto Dental University, Nagano, Japan

3 Department of Oral and Maxillofacial Radiology, Institute of Biomedical and Health Science, Hiroshima University, Hiroshima, Japan

fractures. However, because of limited numbers of facilities and trained personnel, it is impossible to apply DXA to all postmenopausal women who are potentially at risk of having low BMD and/or fractures [10].

Previous studies have suggested that panoramic radiography may be a useful tool to identify postmenopausal women with low skeletal BMD [11–16]. In particular, several studies have indicated that a linear radiolucent image of the endosteal margin of the lower border of the mandible (just under or distal to the mental foramen) on panoramic radiographs is a consequence of diminished skeletal BMD [11–13, 15, 16]. Based on these reports, a computer-aided diagnosis (CAD) system to identify patients with osteoporosis using panoramic radiographs was first developed at our institution [17]. This system can readily detect the linear radiolucent image within the inferior border of the mandibular cortex on panoramic radiographs. Cortical changes are particularly evident in patients with low BMD. Although this CAD system has high diagnostic accuracy, most steps in extracting the region of interest (ROI) must be performed manually. In addition, because the ROI sample size is limited (100 × 100 pixels), cortical bone with linear radiolucent images is likely to go unnoticed. As shown in Fig. 1, if the linear bone resorption image is not included because of the small ROI, it may not be possible to reach an accurate diagnosis. The aims of this study were to expand the size of the ROI to reduce the risk of missing the area, where the linear radiolucent images are seen and to semi-automatize both extraction and selection of the ROI, so that operation time and complexity can be reduced in comparison with our previous CAD system. We also measured and compared the diagnostic performance of the new system with that of the conventional system.

All authors declare that they have no conflict of interest. All procedures followed were in accordance with the ethical standards of the responsible committee on human experimentation (institutional and national) and with the Helsinki Declaration of 1975, as revised in 2008 (5). Informed consent was obtained from all patients for being included in the study.

Materials and methods

Panoramic radiographs and BMD assessment

Two hundred postmenopausal women aged ≥ 50 years who visited the outpatient clinic of Oral and Maxillofacial Radiology at Hiroshima University Hospital from 2009 to 2011 were the subjects of this study. All women were given a detailed explanation of the research and provided informed consent before enrollment. No patients had metabolic bone disease, cancer with bone metastasis, or major renal impairment, and no patients were taking any medications that could affect bone metabolism. Panoramic radiographs of all patients were taken using Cypher® digital panoramic X-ray equipment (Asahi Roentgen, Kyoto, Japan). All panoramic radiographic images were 2876 × 1536 pixels in size. Of these 200 images, 100 were used to estimate the most suitable reference point for automatic extraction of the ROIs and to calculate a threshold value to discriminate between noise and proper bone after image processing (Group A),

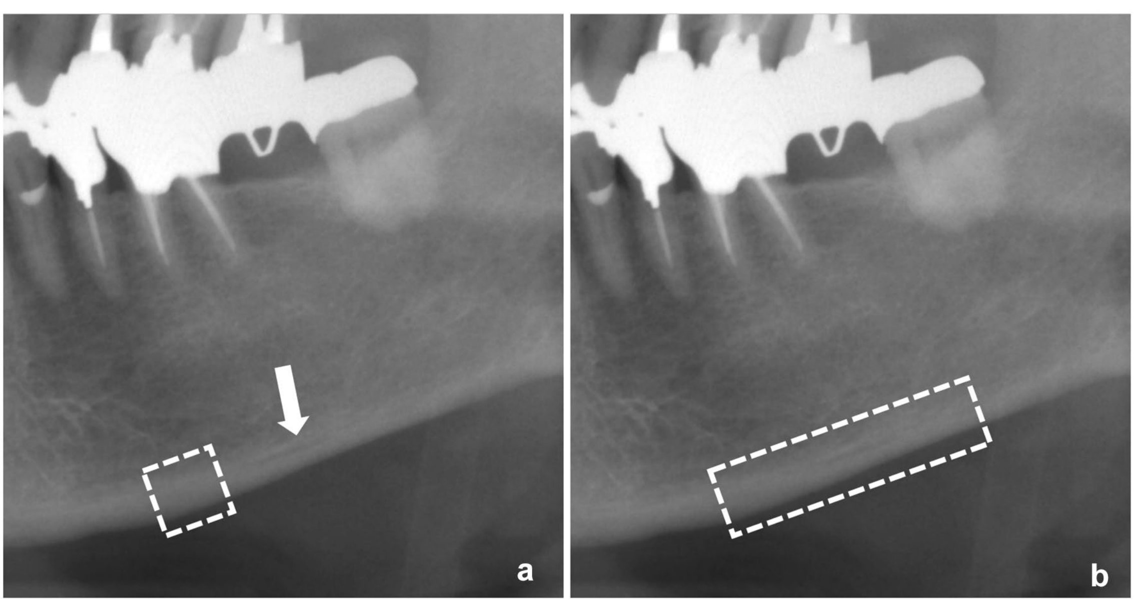

Fig. 1 Comparison of the conventional small region of interest (ROI) and the newly created large ROI. **a** Conventional ROI does not include the part containing the bone structural change (arrow). **b** New large ROI includes the area of structural change

and 100 images were used to confirm the diagnostic performance of the system (Group B). BMD measurements of the lumbar spine (L2–L4) were performed for all 200 patients using DXA (DPX-alpha; Lunar Co., Madison, WI, USA). The absence of vertebral fractures was also confirmed in all patients using lateral radiographs of the lumbar spine taken at the same time as the DXA measurement. Based on the World Health Organization classification, low skeletal BMD was defined as a BMD *T* score of − 1.0 or less. The presence of osteoporosis was defined as a BMD *T* score of − 2.5 or less [18]. The distribution of skeletal BMD data is shown in Table 1. The rate of patients with osteoporosis in the present study was very similar to that in a different group of postmenopausal women aged ≥ 50 years in a Japanese cohort study investigating healthy adults [19].

Semi-automatization of ROI processing and construction of a diagnostic program

To simplify the operation of the system and shorten the operation time, the selection of ROI was automated as much as possible. The CAD software was programmed in MATLAB 2010a in combination with the Image Processing Toolbox (MathWorks, Inc. Natick, MA, USA). The ROI must include the lower border of the mandible just under or distal to the mental foramen [11, 12]. Without any reference point, it is difficult for the computer to identify the location. First, an optimized reference point was needed for subsequent semi-automatic extraction and processing of the large ROI. To estimate this reference point, 14 dental practitioners (mean age, 48.5 years; mean clinical experience, 23.7 years) were asked to delineate the inferior border of the mandible immediately under the mental foramen within all Group A images. The average value of all specified coordinates was then calculated and defined as the optimal reference point (point 1 in Fig. 2). The coordinates on the contour edge line, which was extracted by a Canny edge detector (which locates edges by looking for local maxima within specific gradients) [20], were subsequently defined as the second reference point (point 2 in Fig. 2). Next, a region of 400 × 100 pixels (the ROI) was automatically extracted along the contour of the mandible using the second reference point. To make it easier

Table 1 Patient characteristics

	Group A	Group B
Mean age and SD (in years)	64.5 ± 8.1	59.5 ± 7.8
Mean BMD *T* score (and SD)	− 1.10 ± 1.49	− 1.15 ± 1.69
BMD *T* score distribution		
BMD *T* score ≥ −1.0 (normal skeletal BMD)	49	51
BMD *T* score < −1.0 (low skeletal BMD[a] or osteoporosis[a])	51	49
BMD *T* score < −2.5 (osteoporosis[a])	23	25

The number of BMD *T* scores of less than − 1.0 also includes the number of BMD *T* scores of less than − 2.5. Therefore, the sum of BMD *T* scores of less than − 1.0 and greater than or equal to − 1.0 is 100, which is the total number of patients

BMD bone mineral density, *SD* standard deviation

[a]Diagnostic criteria of low skeletal BMD and osteoporosis are based on the World Health Organization definition

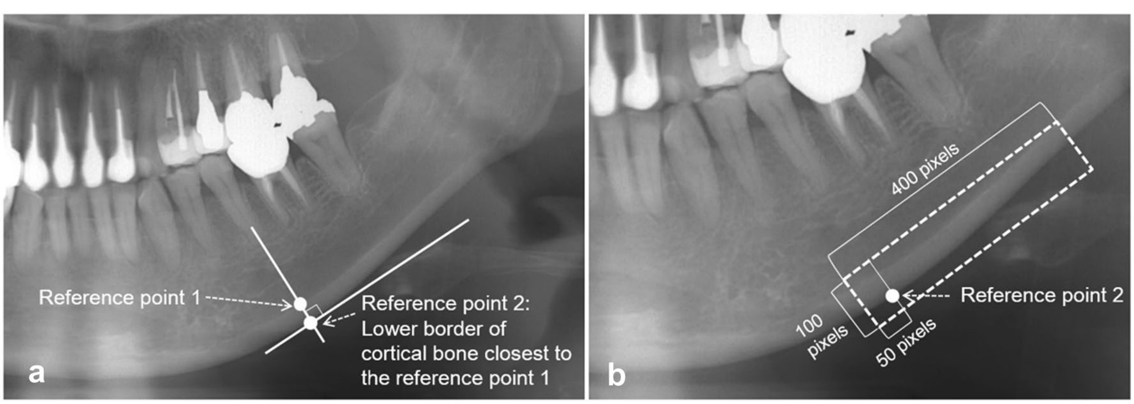

Fig. 2 Overview of image processing for region of interest (ROI) extraction. **a** Reference point 2 is defined as the point perpendicularly below or above reference point 1. **b** Region of 400 × 100 pixels was extracted as the ROI along the contour of the mandible from the 50-pixel mesial coordinate of reference point 2

to specify any non-analyzable parts for exclusion from the diagnosis, the larger 400 × 100-pixel ROI was divided into four 100 × 100-pixel blocks. Among these blocks, the operator running the CAD program then judged and excluded any block containing variations that did not adhere to the mandibular cortical bone region. Only selected blocks could be further examined using one of the two novel diagnostic programs. To illustrate this, Fig. 3 shows some examples of block selection within a larger ROI. If the mandibular cortical bone could not be extracted correctly, all blocks of the ROI were excluded.

Subsequent diagnostic analysis was performed using two different methods that consisted of their own program in MATLAB. The first method (program 1) was to treat each block separately and run an analysis similar to the previous conventional CAD method [17]. The second diagnostic program (program 2) was designed to allow for a more precise analysis in either contiguous or standalone blocks by scanning through the target area in a detailed fashion of about 10 pixels per iteration. One clear advantage of program 2 is that it can scan across borders between adjacent selected blocks and take this information into account.

Similar to the previously available CAD system, all images included in the areas suitable for further analysis were binarized (i.e., assigned one of the two color values) after extracting a morphological skeleton based on several mathematical morphological parameters [16, 21]. In particular, using the Group A images, the threshold value (pixel size) that distinguished between the generated skeleton line(s) and the noise was obtained in the following way. For all selected blocks, the line element size (in pixels) generated in all ROI blocks without overlapping structures (such as the hyoid bone) of Group A images was analyzed by examining its frequency distribution (Fig. 4). In total, 619 of 800 blocks extracted from Group A images contained no unwanted structures on any side. Small-size line elements (e.g., < 10 pixels; large peak) constituted the main bulk. This part mainly included small pixels which were considered as noise. Accordingly, the upper 95th percentile value of this group (92 pixels) was determined as the threshold value between skeleton lines that should be evaluated and noise. Previous studies have shown that linear radiolucent images appear in the mandibular cortical bone of patients with low BMD [11, 13, 15, 17]. In other words, in subjects with low predicted skeletal BMD, cortical bone is divided into multiple structures by linear bone resorption images. Therefore, after image processing, the image is converted into multiple skeleton lines. However, in subjects with normal predicted BMD, because a linear radiolucent image is not seen inside the cortical bone, the image of cortical bone is converted

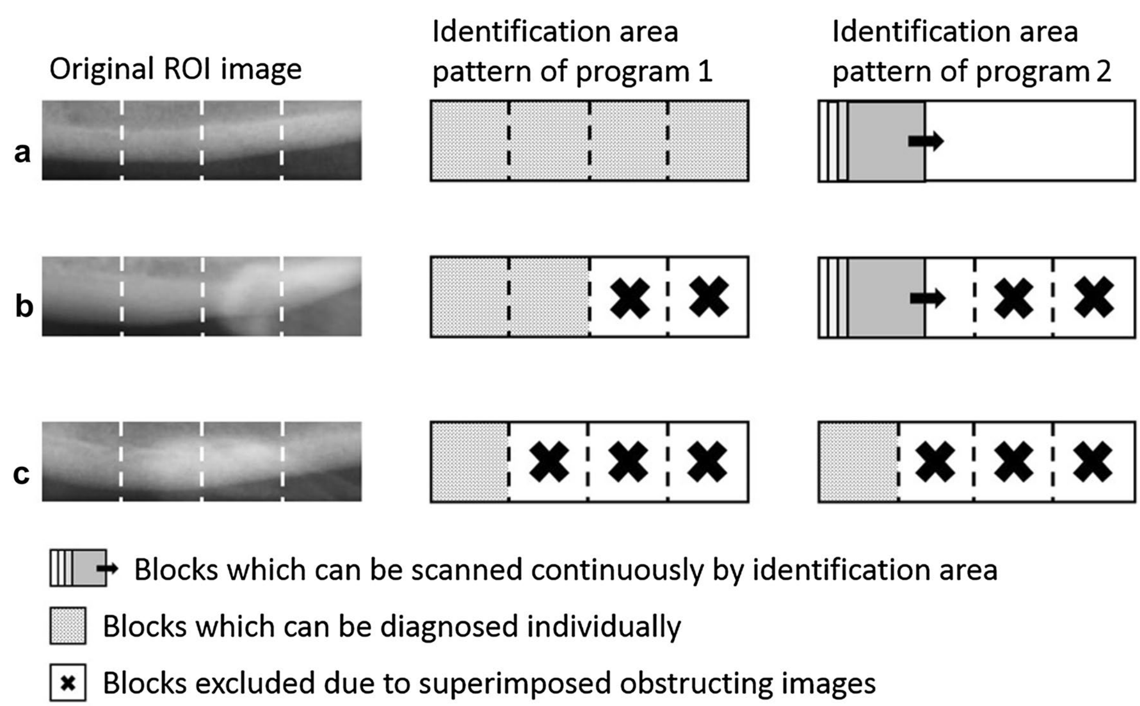

Fig. 3 Division of the region of interest into four blocks of 100 × 100 pixels. **a** If no blocks are to be excluded, all four blocks can be evaluated by programs 1 and 2. Program 2 can scan inside all blocks by scanning the identification area. **b** Only two blocks can be evaluated (the other two blocks must be excluded because of superimposition of the hyoid bone image). Program 2 can scan inside the two blocks. **c** If no contiguous blocks are present because of the excluded blocks, each block is individually diagnosed. In such a case, scanning the identification area cannot be performed by program 2

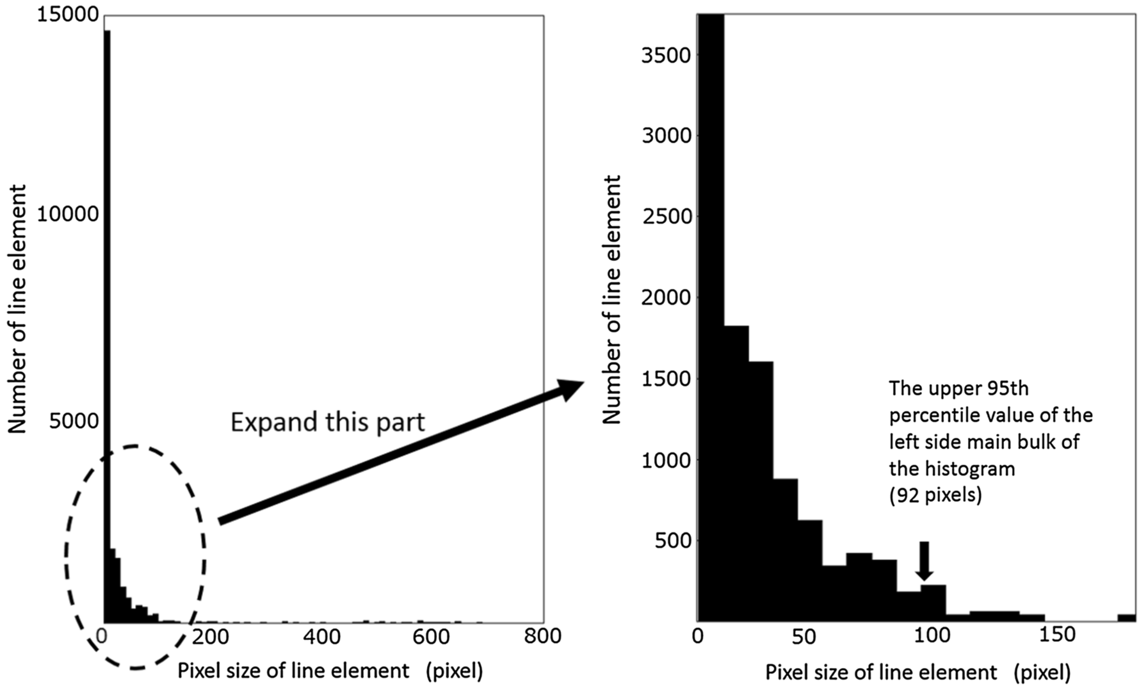

Fig. 4 Histogram showing the sizes of all line elements generated in the regions of interest of group A images. Small-size line elements (e.g., < 10 pixels; large peak) constitute the main bulk. The upper 95th percentile value of this group (92 pixels) was determined as the threshold value that distinguished between skeleton lines that should be evaluated and noise

into only one skeleton line. Based on this theory, if any images within the blocks divided into two or more skeleton lines after noise exclusion, the system would diagnose the patient as being likely to have low skeletal BMD or even osteoporosis (Fig. 5). Figure 6 shows a flow diagram from ROI extraction to diagnosis.

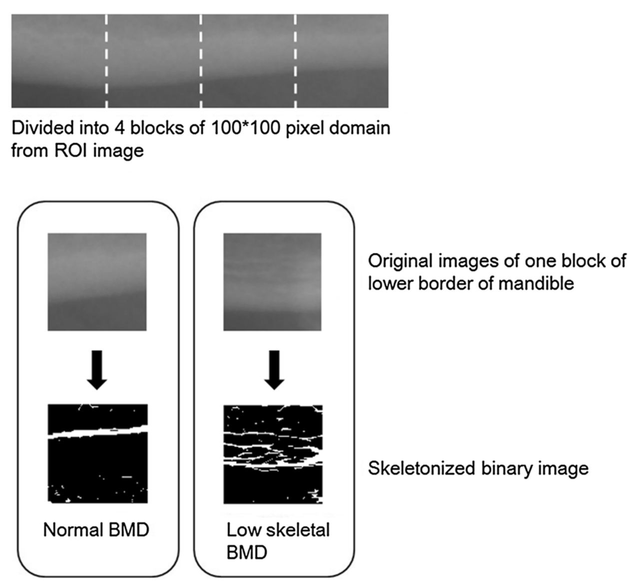

Fig. 5 Image processing result for patients expected to have normal and low BMD. In subjects with normal predicted BMD, no linear radiolucent image is seen inside the cortical bone. Therefore, because only one structure is seen inside the divided block, the image is converted into one skeleton line by image processing. In subjects with low BMD, the original image of the cortical bone is converted into multiple skeleton lines, since it is divided into multiple structures by linear radiolucent images

Calculation of the rate of ROIs that could be extracted correctly and blocks that could be evaluated

We calculated the rate of ROIs correctly extracted from the lower mandibular cortical bone. As shown in Fig. 3, we also calculated the rate at which blocks could be evaluated without being deleted because of the inclusion of unnecessary images, such as the hyoid bone.

Comparison of diagnostic performance and operation time between the conventional diagnostic program and the two novel diagnostic programs 1 and 2

To evaluate the diagnostic performance between the previous CAD program and the two novel CAD programs, the sensitivity, specificity, positive predictive value, negative predictive value, and accuracy were calculated using dichotomous 2 × 2 tables. These tables were obtained from both

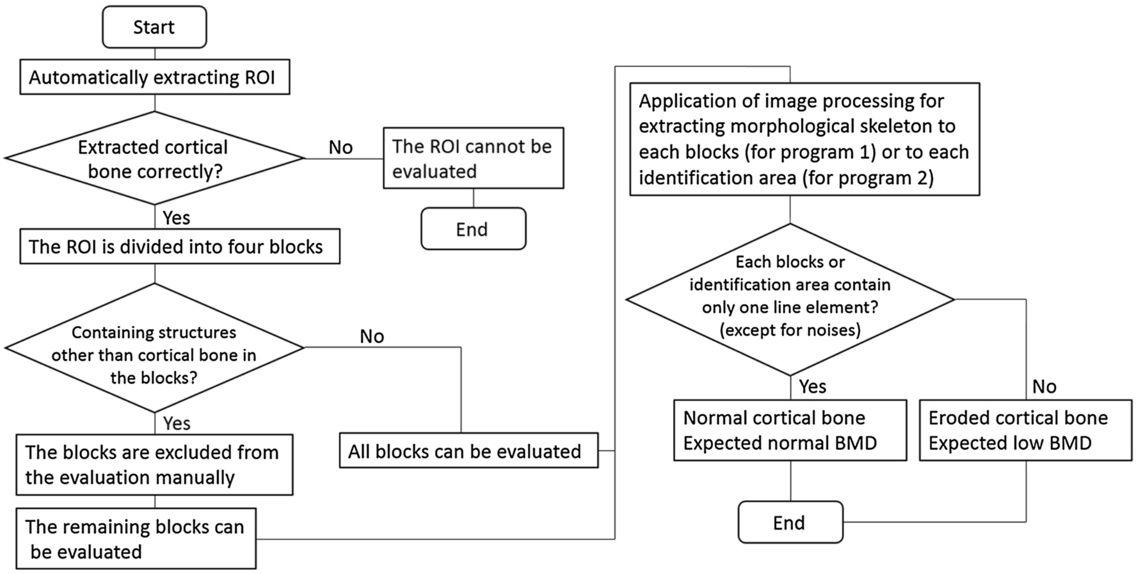

Fig. 6 Flow diagram of the novel systems from region of interest extraction to diagnosis

the diagnostic information based on BMD assessment of the lumbar spine and the results of the diagnostic programs themselves. We used SPSS v11.0 statistical software (SPSS Inc., Chicago, IL, USA) for these statistical evaluations. The calculated values of the new CAD software based on program 1, program 2, and the previous conventional system were then compared. When the 95% confidence intervals for each measurement did not overlap, a significant difference was considered to exist between them. The overall time taken to diagnose all 100 Group B images using all three programs was also measured. All programs were operated by the first author (TN; clinical experience of 16 years), and the same diagnostic and medical equipment, including the computer on which all programs were run (Windows 8.1 Enterprise 64-bit, Intel Core i7-4770 3.4 GHz CPU, 16 GB RAM), was used for these evaluations.

Results

The novel CAD software automatically extracted the lower border of the mandible (400 × 100 pixels) within 194 ROIs (97.0%) of all 200 potentially extractable ROIs (i.e., both left and right sides of the mandible within all 100 radiographs of Group B). In total, 636 of 800 blocks extracted from Group B images contained no unwanted structures, such as the hyoid bone, on any side. In addition, 48% of all 100 cases in Group B could be diagnosed fully automatically without significant operator intervention. However, in six ROIs (3.0%), the lower border of the mandible was not extracted correctly. An example is shown in Fig. 7. In these cases, structures with higher radiopacity than usual are located near the cortical bone. The diagnostic performances are shown in Table 2. Of the two newly developed CAD programs, the precise scanning method inside and across consecutive blocks (program 2) displayed the highest sensitivity. However, owing to a higher false-positive rate, the specificity of program 2 was slightly lower than that of program 1 and the conventional program. In the cases of false positives in program 2, slight bone structure changes were detected. However, in the cases of false negatives in both the old and new systems, it was seen that the skeleton lines after image processing were connected to one another and converted into a single pixel agglomeration. An example is shown in Fig. 8. The time required for operation and diagnosis was 43 min 28 s for the conventional program, 22 min 21 s for program 1, and 30 min 8 s for program 2. Therefore, compared with the conventional system, the operation time decreased to 51.4% for program 1 and 69.3% for program 2.

Discussion

For most panoramic radiographs used in this study, the ROIs could be extracted automatically with high validity. However, in six ROIs (3.0%), the lower border of the mandible was not extracted correctly. If structures with higher radiopacity than usual are located near the cortical bone and if reference point 1 of Fig. 1 is close to the images of such high radiopacities, it is possible that the system may misinterpret them as being cortical bone, because such high opacity images are similar to the image of the mandibular cortical bone. Further studies are needed to reduce such potential misinterpretations. However, even for these cases, a suitable

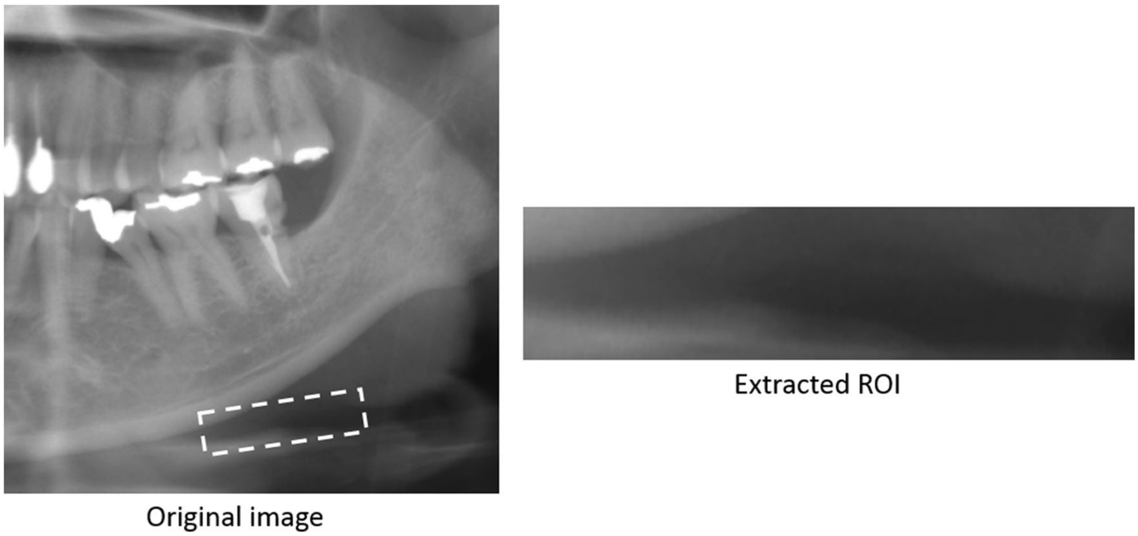

Fig. 7 Example of a case in which the upper border of the hyoid bone was mistakenly extracted as a region of interest. If structures with higher radiopacity than usual are located near the cortical bone, the system may misinterpret them as being cortical bone

Table 2 Comparison of diagnostic performance for identifying patients in Group B with low skeletal BMD (or osteoporosis) between the novel and conventional computer-aided diagnosis systems

	Sensitivity % (95% CI)	Specificity % (95% CI)	Positive predictive value % (95% CI)	Negative predictive value % (95% CI)	Accuracy % (95% CI)
Novel system					
Program 1					
BMD *T* score < −1.0 (low skeletal BMD)	65.3 (56.0–74.6)	74.5 (65.9–83.0)	71.1 (62.2–80.0)	69.1 (60.0–78.2)	70.0 (61.0–79.0)
BMD *T* score < −2.5 (osteoporosis)	84.0 (76.8–91.2)	68.0 (58.9–77.1)	46.7 (36.9–56.5)	92.7 (87.6–97.8)	72.0 (63.2–80.8)
Program 2					
BMD *T* score < −1.0 (low skeletal BMD)	71.4 (62.5–80.3)	68.6 (59.5–77.7)	68.6 (59.5–77.7)	71.4 (62.5–80.3)	70.0 (61.0–79.0)
BMD *T* score < −2.5 (osteoporosis)	92.0 (86.7–97.3)	62.7 (53.2–72.2)	45.1 (35.3–54.9)	95.9 (92.0–99.8)	70.0 (61.0–79.0)
Conventional system					
BMD *T* score < −1.0 (low skeletal BMD)	61.2 (51.6–70.6)	70.6 (61.7–79.5)	66.7 (57.5–75.9)	65.5 (56.2–74.8)	66.0 (56.7–75.3)
BMD *T* score < −2.5 (osteoporosis)	80.0 (72.2–87.8)	66.7 (57.5–75.9)	44.4 (34.7–54.1)	90.9 (85.3–76.5)	70.0 (61.0–79.0)

BMD bone mineral density, *CI* confidence interval

ROI could still be correctly extracted on the contralateral side. Therefore, even if a suitable ROI is extracted on only one side, individuals at risk of low BMD or osteoporosis can still be identified.

Because automated extraction of widened ROIs has been successfully deployed in the novel CAD program, the chance that morphological changes outside shorter ROIs (as used in the conventional system) would go undetected has significantly diminished. Among the cases in which the cortical bone was correctly included in the ROI, four ROIs could not be analyzed using the conventional CAD system because of the previous ROI size limit, as shown in Fig. 1 (i.e., the area of interest was outside the conventional CAD system operating parameters). Using the novel CAD system and the two new diagnostic programs, there were no such limits for the Group B data set.

In addition, although no significant difference was observed, the sensitivity was slightly higher than that

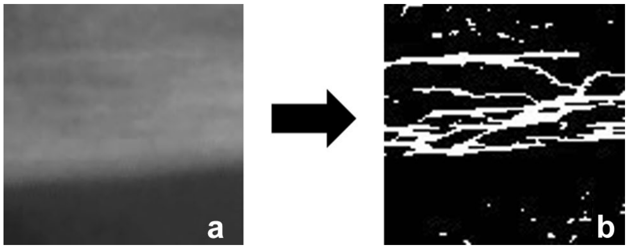

Fig. 8 Example of a case in which all skeleton lines were connected when image processing was performed. **a** Because a linear radiolucent image was observed in the cortical bone, low bone density was predicted. **b** Mathematical morphological skeleton line of image A was extracted. All lines are connected

of the conventional program. Furthermore, program 2, which actively scans the inside of the ROI (and across borders) in small increments, aptly identified several people as "suspected to have low BMD" and displayed excellent sensitivity. In the diagnosis of osteoporosis (BMD *T* score < − 2.5), the decrease in specificity (− 4.0%) was somewhat less than the increase in sensitivity of program 2 (+ 12%) compared with the conventional system. Therefore, the novel system using program 2 can find low BMD patients more efficiently than the conventional system. However, the number of false positives also increased, because particular cases with only slight bone structure changes were also judged as "suspected to have low BMD". In the current CAD version, the final diagnostic conclusion is occasionally the same for a variety of empirical results. For example, for cases in which only two skeleton lines are present, and which are found only in one block of the ROI, as well as in cases in which a more prominent number of skeleton lines is found in multiple blocks, the final verdict of the system would be "suspected low BMD". Conversely, as shown in Fig. 8, a rare problem is that sometimes all the skeleton lines are connected to one another. Consequently, they are converted into a single pixel agglomeration; that is, the number of skeletal lines (other than noise) is erroneously counted as "1". Therefore, although this is clearly a case of low BMD, the image in this rare case was not interpreted as positive. To obtain higher diagnostic accuracy, we must take into account not only the number of skeleton lines as a result of mathematical morphological image processing but also the form of the skeleton lines, such as the perimeter of all skeletal lines. Several studies have shown that the thickness of the lower border of the mandibular cortical bone is also a useful diagnostic tool when predicting the presence of low BMD [11, 14, 22–26]. A further study that includes cortical thickness would be necessary to improve the diagnostic efficacy of CAD systems in the future. In the current CAD version, the software can only display whether low BMD is *suspected*. Therefore, clinicians might benefit from the possibility of linking the diagnostic result to a meaningful numerical value such as a "mandibular margin morphology index" during the diagnostic presentation.

In addition, in the novel CAD software, the time required for diagnosis was meaningfully shortened, and staff efforts to operate the system were significantly reduced. Because the method of operation in program 2 (i.e., scanning in 10-pixel increments) involved the same number of processing steps as in program 1, the final diagnosis took somewhat longer. Even so, program 2 could still reach its final diagnosis within a much shorter time span than the conventional system.

Compared with our previous study, the conventional system exhibited good reproducibility, although there were some minor discrepancies [17]. However, the novel system seems to allow for wider reproducibility, given that the operator, when necessary, can aptly select and remove all blocks containing structures other than cortical bone. Whether reproducibility is also excellent when the same patient is investigated multiple times is unknown; this is difficult to assess because of the ethical problems that arise when taking multiple X-ray images of the same patient without necessary medical grounds. A potential solution may be to investigate replicability using dry skull images.

Finally, the algorithm used by the CAD system must be modified, so that it can accommodate a larger range of panoramic X-ray equipment. For example, the reference point coordinates in this study can only be used in combination with radiographs taken by Cypher® digital panoramic X-ray equipment or compatible machines with a resolution of 300 dpi and 2876 × 1536 pixels in size. Other image characteristics, such as contrast and granularity, may also vary depending on the X-ray equipment. Therefore, amending some of the aforementioned pitfalls, implementing new features, and developing a general data processing module that makes the CAD system deployable on a variety of X-ray equipment will allow for more widespread use of the CAD software in general clinical practice. This will allow clinicians worldwide to use this new method to identify asymptomatic patients with low BMD or osteoporosis at an earlier stage.

In conclusion, for most of the panoramic radiographs (97%), larger-sized ROIs could be extracted automatically. The sensitivity of the novel CAD system for identifying subjects with low BMD was slightly improved. Because the operation of the system was semi-automated, the CAD system can be used without complicated operations. With continued development of the CAD diagnostic tool, patients at risk of low skeletal BMD will be identified more rapidly and efficiently, leading to earlier detection and intervention.

Compliance with ethical standards

Conflict of interest Nakamoto T, Taguchi A, Verdonschot RG, and Kakimoto N declare that they have no conflict of interest.

Human rights statement and informed consent All procedures followed were in accordance with the ethical standards of the responsible committee on human experimentation (institutional and national) and with the Helsinki Declaration of 1975, as revised in 2008 (5). Informed consent was obtained from all patients for being included in the study.

Animal rights statement This article does not contain any studies with animal subjects performed by the author.

References

1. Dervis E. Oral implications of osteoporosis. Oral Surg Oral Med Oral Pathol Oral Radiol Endod. 2005;100:349–56.
2. International Osteoporosis Foundation. Report on Japan, Asia-Pacific regional audit. 2013. http://www.iofbonehealth.org/sites/default/files/media/PDFs/Regional%20Audits/2013-Asia_Pacific_Audit-Japan_0_0.pdf. Cited 28 Nov 2017.
3. World Health Organization. Assessment of fracture risk and its application to screening for postmenopausal osteoporosis. Report of a WHO Study Group. World Health Organ Tech Rep Ser. 1994;843:94–101.
4. Lydick E, Cook K, Turpin J, Melton M, Stine R, Byrnes C. Development and validation of a simple questionnaire to facilitate identification of women likely to have low bone density. Am J Manag Care. 1998;4:37–48.
5. Weinstein L, Ullery B. Identification of at-risk women for osteoporosis screening. Am J Obstet Gynecol. 2000;183:547–9.
6. Cadarette SM, Jaglal SB, Kreiger N, Mclsaac WJ, Darlington GA, Tu JV. Development and validation of the osteoporosis risk assessment instrument to facilitate selection of women for bone densitometry. CMAJ. 2000;162:1289–94.
7. Koh LKH, Sedrine WB, Torralba TP, Kung A, Fujiwara S, Chan SP, Huang QR, Rajatanavin R, Tsai KS, Park HM, Reginster JY. Osteoporosis self-assessment tool for Asians (OSTA) Research Group. A simple tool to identify Asian women at increased risk of osteoporosis. Osteoporos Int. 2001;12:699–705.
8. Fujiwara S, Masunari N, Suzuki G, Philip DR. Performance of osteoporosis risk indices in a Japanese population. Curr Ther Res. 2001;62:586–94.
9. Miller PD, Siris ES, Barrett-Connor E, Faulkner KG, Wehren LE, Abbott TA, et al. Prediction of fracture risk in postmenopausal white women with peripheral bone densitometry: evidence from the National Osteoporosis Risk Assessment. J Bone Miner Res. 2002;17:2222–30.
10. Kanis JA, Johnell O. Requirements for DXA for the management of osteoporosis in Europe. Osteoporos Int. 2005;16:229–38.
11. Taguchi A, Suei Y, Ohtsuka M, Otani K, Tanimoto K, Ohtaki M. Usefulness of panoramic radiography in the diagnosis of postmenopausal osteoporosis in women. Width and morphology of inferior cortex of the mandible. Dentomaxillofac Radiol. 1996;25:263–7.
12. Devlin H, Horner K. Mandibular radiomorphometric indices in the diagnosis of reduced skeletal bone mineral density. Osteoporos Int. 2002;13:373–8.
13. Nakamoto T, Taguchi A, Ohtsuka M, Suei Y, Fujita M, Tanimoto K, et al. Dental panoramic radiograph as a tool to detect postmenopausal women with low bone mineral density: untrained general dental practitioners' diagnostic performance. Osteoporos Int. 2003;14:659–64.
14. Lee K, Taguchi A, Ishii K, Suei Y, Fujita M, Nakamoto T, et al. Visual assessment of the mandibular cortex on panoramic radiographs to identify postmenopausal women with low bone mineral densities. Oral Surg Oral Med Oral Pathol Oral Radiol Endod. 2005;100:226–31.
15. Devlin H, Karayianni K, Mitsea A, Jacobs R, Lindh C, van der Stelt P, et al. Diagnosing osteoporosis by using dental panoramic radiographs: the OSTEODENT project. Oral Surg Oral Med Oral Pathol Oral Radiol Endod. 2007;104:821–8.
16. Passos JS, Gomes Filho IS, Sarmento VA, Sampaio DS, Gonçalves FP, Coelho JM, et al. Women with low bone mineral density and dental panoramic radiography. Menopause. 2012;19:704–9.
17. Nakamoto T, Taguchi A, Ohtsuka M, Suei Y, Fujita M, Tsuda M, et al. A computer-aided diagnosis system to screen for osteoporosis using dental panoramic radiographs. Dentomaxillofac Radiol. 2008;37:274–81.
18. Kanis JA, WHO Study Group. Assessment of fracture risk and its application to screening for postmenopausal osteoporosis: synopsis of a WHO report. Osteoporos Int. 1994;4:368–81.
19. Orimo H, Nakamura T, Hosoi T, Iki M, Uenishi K, Endo N, et al. Japanese 2011 guidelines for prevention and treatment of osteoporosis—executive summary. Arch Osteoporos. 2012;7:3–20.
20. Canny JF. A computational approach to edge detection. IEEE Trans Pattern Anal Mach Intell. 1986;8:679–98.
21. Soille P. Morphological image analysis: principle and applications. 2nd ed. Berlin: Springer; 2003.
22. Arifin AZ, Asano A, Taguchi A, Nakamoto T, Ohtsuka M, Tsuda M, Kudo Y, Tanimoto K. Computer-aided system for measuring the mandibular cortical width on dental panoramic radiographs in identifying postmenopausal women with low bone mineral density. Osteoporos Int. 2006;17:753–9.
23. Kavitha MS, Asano A, Taguchi A, Kurita T, Sanada M. Diagnosis of osteoporosis from dental panoramic radiographs using the support vector machine method in a computer-aided system. BMC Med Imaging. 2012;12:1. https://doi.org/10.1186/1471-2342-12-1.
24. Kavitha MS, Samopa F, Asano A, Taguchi A, Sanada M. Computer-aided measurement of mandibular cortical width on dental panoramic radiographs for identifying osteoporosis. J Investig Clin Dent. 2012;3:36–44.
25. López-López J, Alvarez-López JM, Jané-Salas E, Estrugo-Devesa A, Ayuso-Montero R, Velasco-Ortega E, et al. Computer-aided system for morphometric mandibular index computation (using dental panoramic radiographs). Med Oral Patol Oral Cir Bucal. 2012;17:624–32.
26. Muramatsu C, Matsumoto T, Hayashi T, Hara T, Katsumata A, Zhou X, et al. Automated measurement of mandibular cortical width on dental panoramic radiographs. Int J Comput Assist Radiol Surg. 2013;8:877–85.